Cellulose (2024) 31:6225–6239
https://doi.org/10.1007/s10570-024-05983-w

ORIGINAL RESEARCH

Nanoprecipitation to produce hydrophobic cellulose nanospheres for water-in-oil Pickering emulsions

Bryan Andres Tiban Anrango · Mohinder Maheshbhai Naiya · Josh Van Dongen · Olivia Matich · Catherine P. Whitby · Jack L.-Y. Chen

Received: 5 March 2024 / Accepted: 23 May 2024 / Published online: 12 June 2024

Abstract In recent years, there has been growing interest in replacing petroleum-based water-in-oil (W/O) emulsifiers with sustainable and less toxic natural materials. Pickering emulsifiers are considered well-suited candidates due to their high interfacial activity and the ability to form emulsions with long-term stability. However, only sporadic examples of natural materials have been considered as inverse Pickering emulsifiers. This study describes the synthesis of a series of hydrophobic cellulose nanospheres by bulk modification with acyl groups of different chain lengths followed by nanoprecipitation, and their application as inverse emulsifiers. Modification with acyl groups of longer chain length (C16, C18) afforded lower degrees of substitution, but resulted in greater thermal stability than groups with shorter acyl chains (C12, C14). Formation of nanospheres with low aspect ratios and narrow size distributions required low initial cellulose concentrations (< 1% w/v), high volumetric ratios of anti-solvent to solvent (> 10:1), and slow addition rates (< 20 mL/h). The modified cellulose nanospheres were able to reduce the interfacial tension between water and hexane from 45.8 mN/m to 31.1 mN/m, with an effect that increased with the number of carbons in the added acyl chains. The stearate-modified nanospheres exhibited superhydrophobic behavior, showing a contact angle of 156° ± 4° with water, and demonstrated emulsification performance comparable to the commonly used molecular surfactant sorbitan stearate. Our findings suggest that hydrophobically modified cellulose nanospheres have the potential to be a bio-derived alternative to traditional molecular W/O emulsifiers.

Supplementary Information The online version contains supplementary material available at https://doi.org/10.1007/s10570-024-05983-w.

B. A. Tiban Anrango · M. M. Naiya · J. Van Dongen · O. Matich · J. L.-Y. Chen
Centre for Biomedical and Chemical Sciences, Auckland University of Technology, Auckland 1010, New Zealand

B. A. Tiban Anrango · M. M. Naiya · O. Matich · J. L.-Y. Chen
The MacDiarmid Institute for Advanced Materials and Nanotechnology, Wellington 6140, New Zealand

C. P. Whitby
School of Natural Sciences, Massey University, Palmerston North 4410, New Zealand

J. L.-Y. Chen (✉)
Department of Biotechnology, Chemistry and Pharmaceutical Sciences, Università degli Studi di Siena, Siena 53100, Italy
e-mail: jack.chen@aut.ac.nz

Graphical Abstract

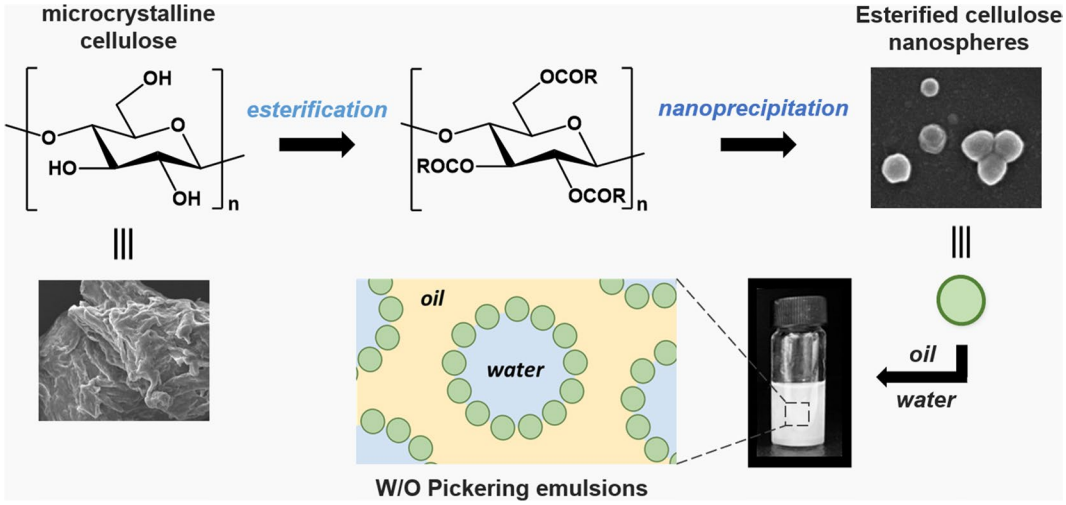

Keywords Spherical cellulose nanoparticles · Inverse Pickering emulsion · Nanoprecipitation · Hydrophobically modified cellulose · Water-in-oil emulsion

Introduction

With a shift towards greener industrial processes, there is growing interest in replacing petroleum-based emulsifiers with sustainable and less harmful natural materials. Pickering emulsifiers are considered promising alternatives due to their high interfacial activity and the capacity to create emulsions with long-term stability. While much work has been performed on the use of natural particles as oil-in-water (O/W) emulsions, there are only sporadic examples of natural particles being used as inverse (water-in-oil; W/O) Pickering emulsifiers. This study explores the use of hydrophobically derivatized cellulose nanospheres for the stabilization of W/O Pickering emulsions.

Pickering emulsions were first described in the early 20th century as particle-stabilized emulsions (Pickering 1907), and their study has considerably increased in the past two decades due to their potential for higher stability compared to surfactant-stabilized emulsions (Aveyard 2012). This characteristic is driven by the adsorption of solid particles to the liquid-liquid interface, creating a physical barrier that prevents droplet coalescence (Gonzalez Ortiz et al. 2020). By accumulating at the interface, the particles lower the interfacial tension between the dispersed and the dispersing phases, allowing the formation of long-stable Pickering emulsions (Levine et al. 1989). One of the key factors that affect the stability of particles at the interface is their wettability (He et al. 2013). Previous research has shown that hydrophilic particles (with contact angles from 15° to 90°) prefer the interfacial curvature of O/W emulsions since they are predominantly immersed in the aqueous phase. On the other hand, particles with greater contact angles (90° to 165°) are more likely to stabilize W/O emulsions (de Carvalho-Guimarães et al. 2022). However, if the system is forced into a state of high total interfacial energy due to high dispersed volume ratios, the emulsion may experience catastrophic phase inversion resulting in the desorption of the particles from the interface and coalescence (Binks and Lumsdon 2000). The morphology of the particles can also alter the nature of interactions at the interface which directly impacts the formation and stability of Pickering emulsions (Yang et al. 2017b). For instance, particles with different aspect ratios such as spheres (Zhang et al. 2023), rods (Daware and Basavaraj 2015; Kalashnikova et al. 2013), discs (Ashby and Binks 2000), fibrils (Silva et al. 2020), and cubes (de Folter et al. 2013) have all been studied and show different mechanisms of self-assembly

at the interface. The effect of differently shaped particles on emulsion stability is still at a nascent stage (Anjali and Basavaraj 2018), and to date, W/O Pickering emulsions have not yet been investigated using hydrophobic spherical cellulose particles. Another important parameter is particle size, which greatly impacts the desorption energy and the number of particles required to form stable emulsions. In general, particles with smaller sizes (< 500 nm) result in higher stabilities due to fast adsorption kinetics from the bulk to the interface, and more effective coverage of the dispersed medium by the particles (Wu and Ma 2016; Lin et al. 2003).

Research on Pickering emulsifiers to date has tended to focus on the formation of O/W emulsions, rather than W/O emulsions due to the vast availability of hydrophilic particles such as silica (Zhang et al. 2023; Binks and Whitby 2004), clay (Ashby and Binks 2000), and magnetite (Yang et al. 2017a) as well as bio-based particles such as chitosan (Meng et al. 2023), starch (Tan et al. 2012; Zhu 2019) and cellulose (Dong et al. 2021; Liu et al. 2020; Kalashnikova et al. 2011; Cherhal et al. 2016; Li et al. 2018; Niu et al. 2018; Costa et al. 2021; Deng et al. 2022; Rehman et al. 2024). The synthesis of particle-based W/O emulsifiers has been dominated by non-bioderived materials. For instance, the surface hydrophobization of silica particles with long chain alkyl groups improved their hydrophobicity by increasing their contact angle to 135°, which allowed the particles to stabilize W/O emulsions with water volume concentrations of up to 40% (Fan et al. 2021). Similarly, hydrophobic monodisperse latex particles have been found to enhance the formation of water-in-toluene emulsions (Binks and Lumsdon 2001); these emulsions readily sediment but are stable to coalescence. In recent years, a small number of studies have been carried out using natural materials or their derivatives for application as W/O Pickering emulsifiers. For example, microcrystalline cellulose (MCC) with high aspect ratios have been grafted with stearoyl chloride to tune the particle wettability and stabilize water-in-toluene emulsions. Such particles induced the formation of medium internal phase and high internal phase emulsions with different degrees of emulsification (Pang et al. 2018). However, the study does not provide information about the time-stability of the emulsions which is of high importance when considering the practical use of these particles as Pickering emulsifiers. Other studies have featured the hydrophobic modification of cellulose nanocrystals, but have explored only their effectiveness as O/W emulsifiers rather than W/O emulsification (Tang et al. 2019; Kibbelaar et al. 2022). Guo and co-workers have reported that intercalative modification of cellulose nanocrystals are able to stabilize W/O emulsions via steric effects rather than reduction of surface tension (Guo et al. 2017). Another example is the fabrication of hydrophobic starch spherical nanoparticles, which have been investigated for the stabilization of water-in-ethyl acetate emulsions for the polymerization of N-isopropyl acrylamide (Zhai et al. 2019). Even though these particles showed good immediate emulsification properties for oil fractions down to 0.3–0.4, significant sedimentation was observed 24 h after storage. In summary, much uncertainty still exists around the practical use of bioderived particles for the formation of stable W/O Pickering emulsions.

This study explores the use of hydrophobically derivatized cellulose nanospheres for the stabilization of W/O Pickering emulsions. Rather than using nanocrystals, benefits are expected from the stabilization of emulsions using nanospheres, such as the ability to control the size and morphology through facile cost-effective techniques such as nanoprecipitation (Zhang et al. 2021), and their ability to be densely organized and well-packed at the interface (Xie et al. 2022). Cellulose nanospheres have only been explored within the context of O/W Pickering emulsions due to their natural hydrophilicity (Liu et al. 2020; Dong et al. 2021). In this study, we synthesized a range of esterified cellulose nanospheres (ECS) via nanoprecipitation, allowing for tuning of the oil-wettability and the formation of stable W/O emulsions. The parameters for nanoprecipitation are optimized for the initial esterified cellulose concentration, the addition rate, and the volume of the antisolvent. The ability of the hydrophobic cellulose nanospheres to act as Pickering emulsifiers are investigated over a range of particle concentrations and water/oil ratios. It is hoped that this research will contribute to a deeper understanding of bioderived particle-based emulsifiers and their use as potential replacements for conventional molecular surfactants.

Experimental section

Materials

MCC powder with an average particle size of 20 µm was purchased from Sigma Aldrich. For the bulk esterification of cellulose, lauroyl chloride, myristoyl chloride, palmitoyl chloride, and stearoyl chloride were purchased from AK Scientific and used as received. Anhydrous pyridine was obtained from Sigma-Aldrich. Dichloromethane, ethanol and hexanes were purchased from ECP chemicals and used as received. Deuterated chloroform was purchased from EURISO-TOP and used in the nuclear magnetic resonance (NMR) experiments. Deionized (DI) water was used to form the W/O Pickering emulsions.

Esterification of MCC

MCC (500 mg) was oven-dried at 90 °C for 1 h and flushed with nitrogen. Then, anhydrous pyridine (13.5 equiv., 10 mL) was slowly added under vigorous stirring. The mixture was sonicated for 10 min to facilitate particle dispersion. The required acyl chloride (3.5 equiv.) was added dropwise into the mixture under vigorous stirring. The heterogeneous reaction mixture was further stirred for 5 h at 110 °C. Ethanol (2 mL) was slowly added to quench the reaction. Then, the mixture was dissolved in dichloromethane (20 mL) at 35 °C under sonication. The obtained solution was mixed with 200 mL of ethanol to precipitate the esterified cellulose which was separated by filtration. The precipitate was re-solubilized in dichloromethane (20 mL) at 35 °C under vigorous stirring and washed with 5% aqueous copper sulfate solution and DI water. Finally, the organic phase was separated and evaporated under reduced pressure to obtain the pure esterified cellulose (EC).

Nanoprecipitation of EC

The corresponding esterified cellulose (1 g) [cellulose laurate (EC_C12), cellulose myristate (EC_C14), cellulose palmitate (EC_C16), or cellulose stearate (EC_C18)], was dissolved in dichloromethane (50 mL). Additional dichloromethane was added to obtain particle concentrations of 0.1, 0.5, 1, 2, and 5% w/v. The cellulosic solution was added dropwise into ethanol (the antisolvent) under vigorous stirring and sonication at room temperature. The addition flow rates investigated were 10, 20, 50 and 100 mL/h. Regarding the volumetric proportions of solvent to antisolvent, ratios of 1:1, 1:5, 1:10, 1:20, and 1:50 were investigated. After precipitation of the esterified, the particles were isolated by centrifugation at 7375 × g RCF for 10 min at 25 °C and air-dried.

Preparation of Pickering emulsions

An appropriate mass of the corresponding ECS was mixed with hexane to obtain particle concentrations of 0.05, 0.1, 0.25, 0.5, 1, and 2% w/v (2 mL). The mixture was stirred and sonicated at room temperature until all the material was homogenously dispersed. Then, DI water (0.9 mL) was slowly added and sonicated for 10 min. The emulsions formed with the esterified cellulose before nanoprecipitation (EC) were made using the same procedure. To compare the ability of the various particles to form Pickering emulsions, the emulsification index (EI%) was determined by considering the emulsion height (H_e) and the total height (H_t) of the mixture according to the following equation:

$$EI(\%) = \frac{H_e}{H_t} x100$$

Infrared spectroscopy

The chemical characterization of MCC and EC was carried out by Fourier-transform infrared spectroscopy (FTIR) using a Nicolet iZ10 FTIR (ThermoFisher). The solid materials were analyzed without prior treatment by placing approximately 10 mg on the spectrometer lens. The wavelength was set from 600 cm^{-1} to 4000 cm^{-1} with an average of 64 scans and a resolution of 4 cm^{-1}. The esterification of cellulose was followed by the appearance of characteristic ester peaks at 1750–1735 cm^{-1} (C = O stretch) and 1210–1163 cm^{-1} (C-O stretch).

Nuclear magnetic resonance

Further chemical characterization of the EC was obtained by liquid-state nuclear magnetic resonance (NMR) using a Bruker Ascend 400 NMR (Bruker) spectrometer operating at 400 MHz. The

corresponding EC (10 mg) was dissolved in chloroform-d_3 and the ^{1}H spectra were recorded. This was used to confirm the esterification and to determine the degree of substitution of the EC based on the integration of the resonances associated with the protons of the anhydrous glucose unit (cellulose backbone) and the protons of the terminal -CH_3 group in the alkyl chain according to the following formula (Wen et al. 2017):

$$DS = \frac{7xI_{Cn,H}}{3xI_{AGU,H}}$$

Thermogravimetric analysis

The thermal stability of the EC was determined by thermogravimetric analysis (TGA) using a Q-5000 TA processor (TA Instruments). MCC and the corresponding EC (4 mg) were analyzed on a 100 µL alumina pan with nitrogen gas (30 mL/min) and a temperature ramp of 10 °C /min up to 600 °C.

Scanning electron microscopy

The morphology of the MCC, EC and ECS was imaged by scanning electron microscopy (SEM) using a SU-70 Schottky field emission scanning electron microscope (Hitachi). 0.1% w/v suspensions of the cellulose particles were dispersed in the appropriate volume of ethanol by sonication. Then, 10 µL of the cellulosic suspensions were transferred onto a glass stub and air-dried for at least 12 h. The dried samples were then Pt-coated for 40 s using an E-1045 ion sputter (Hitachi) and imaged at 10 kV.

Dynamic light scattering

The average particle size and size distribution of the ECS were obtained by dynamic light scattering (DLS) using a Zetasizer Nano ZSP (Malvern Instruments). The ECS were dispersed in an appropriate volume of ethanol to obtain a concentration of 0.1% w/v under sonication. The nanosuspensions were analyzed in triplicate at 20 °C with at least 13 measurements in each experiment.

Contact angle

The static water contact angle of the ECS was determined using an Ossila Contact Angle Goniometer (Ossila). Samples of the ECS were prepared by dispersing the corresponding esterified cellulose (100 mg) into 2 mL of hexane. The suspension was placed on a round surface and the hexane was evaporated overnight at room temperature. The obtained pellet was compressed and positioned onto the goniometer holder. A drop of DI water (2 µL) was placed onto the ECS sample and the contact angle was measured after 1 s at room temperature and 80% relative humidity.

Interfacial tension

The interactions between the ECS and the two immiscible liquids in the emulsion were estimated by the water-hexane interfacial tension with an Attension® Sigma 703D tensiometer (Biolin Scientific). The corresponding ester was homogenously dispersed in an appropriate volume of hexane to obtain a concentration of 1% w/v. This suspension was slowly added on top of a similar volume of DI water and the interfacial tension was measured with a platinum Du Nouy ring. Ten replicates were carried out for each sample.

Optical microscopy

A Leica ICC50 W (Leica Microsystems) optical microscope was used to record the dispersed emulsion droplets. The corresponding Pickering emulsion (10 µL) was transferred onto a glass microscope slide and imaged without any further treatment. The droplet size distribution was analyzed by the software Image J.

Results and discussion

Synthesis and characterization of the esterified cellulose (EC)

The bulk esterification of MCC was carried out with a series of acyl chlorides and pyridine in a heterogeneous reaction which turned into a homogenous solution as the cellulose was modified and solubilized (Maim et al. 1951). Successful esterification

was confirmed by characterization using FTIR and NMR, as seen in Fig. 1a and b. The IR spectra showed the incorporation of acyl chains onto the glucose backbone of cellulose, as evidenced by the appearance of strong absorption peaks around 2950 and 2850 cm^{-1}, which are indicative of C-H stretching vibrations from the long alkyl chains and a characteristic peak at 1750 cm^{-1}, attributed to the C=O stretching vibration of the ester group. Both signals are only observed on the modified cellulose. In addition, the absence of the broad absorption from 3050 to 3600 cm^{-1}, ascribed to the O-H stretch, suggests that most of the hydroxyl groups were esterified, indicating a high degree of substitution (Nunes et al. 2020). As the esterified cellulose was fully soluble in $CDCl_3$, the degree of substitution could be confirmed using ^{1}H NMR analysis (Fig. 1b). The proton spectrum of cellulose laurate (EC_C12) showed signals from 3.0 to 5.2 ppm belonging to protons H1 to H6 in the cellulose backbone, while the protons from the added lauroyl chains were observed at 2.25 (H8), 1.46 (H9), 1.19 (H10 to H17), and 0.81 ppm (H18). Similar spectra were obtained for the other esterified celluloses (see Supporting Information, section 1b), with the main variation being the peak intensity at 1.19 ppm due to the different carbon chain lengths. These spectra allowed us to calculate the degree of substitution (DS) of the cellulose esters by comparing the integration of the proton resonances in the AGU and the terminal -CH_3 group of the added acyl chains (SI, section 1c) (Wen et al. 2017). As seen in Fig. 1c, the DS was observed to decrease as the length of the acyl chain increases, from DS of 2.6 for lauroyl chloride to a DS of 2.3 for stearoyl chloride, which reflects the increase in steric effects as the length of the acyl chain increases. To further compare the properties of the EC after incorporation of the alkyl chains, the thermal stability was determined by thermogravimetric analysis (TGA), shown in Fig. 1d. Interestingly, the lauroyl cellulose (EC_C12) and myristoyl cellulose (EC_C14) showed lower thermal stability than MCC (268 °C) with initial decomposition temperatures at

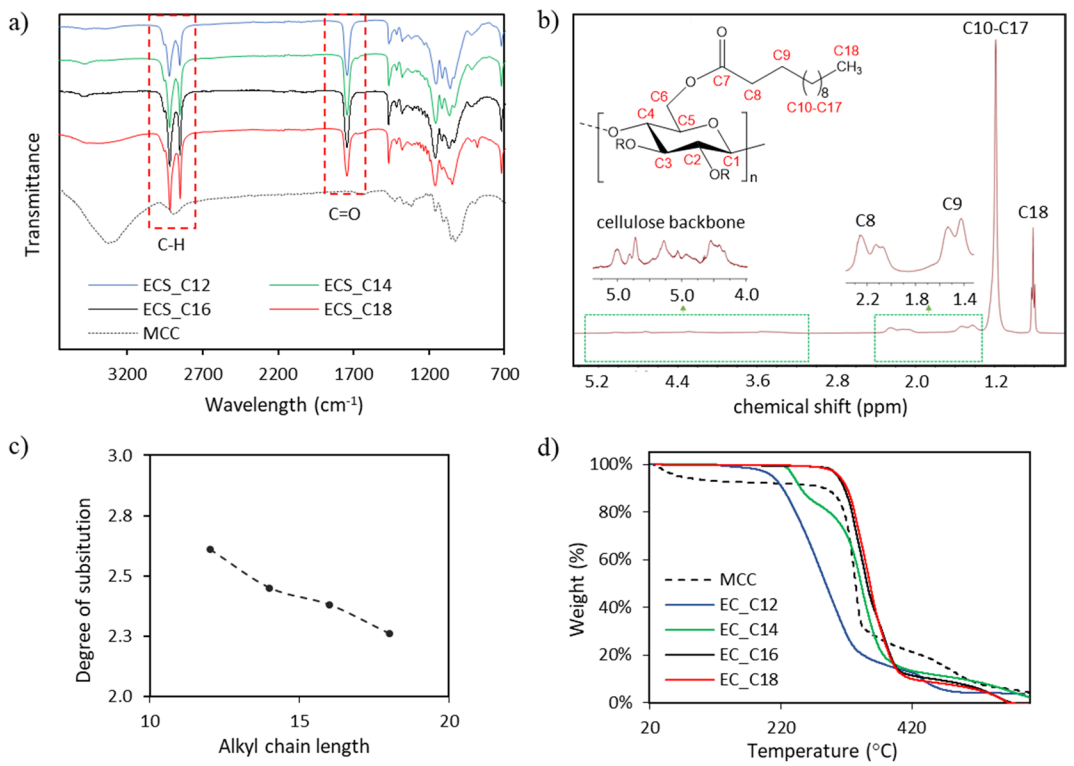

Fig. 1 (**a**) The IR spectra of EC esterified with lauroyl chloride, myristoyl chloride, palmitoyl chloride, and stearoyl chloride. (**b**) The ^{1}H NMR spectra of EC esterified with lauroyl chloride in chloroform-d_3. (**c**) Degree of substitution of the EC (C12-C18). (**d**) TGA of the EC (C12-C18) and MCC

170 °C and 210 °C respectively. On the other hand, the esterified cellulose with longer chains (palmitoyl and stearoyl) exhibited higher thermal stability with initial decomposition temperatures of 276 °C and 279 °C respectively. This is in line with previous reports that showed longer chain lengths afford higher degrees of order, resulting in an increase in the onset temperature of decomposition (Heinze et al. 2016; Huang 2012). Additionally, our esterified particles do not show mass reduction below 100 °C, which is commonly observed with cellulosic structures due to their tendency to absorb water. The absence of this behavior with the EC samples further supports a change in the wettability of the cellulose.

Formation of esterified cellulose nanospheres

Due to the introduction of long acyl chains onto the cellulose structure, the esterified cellulose is soluble in slightly polar organic solvents such as dichloromethane, but insoluble in more polar solvents such as ethanol. This property allowed us to synthesize nanospheres *via* the antisolvent nanoprecipitation technique (Hornig and Heinze 2008; Horn and Rieger 2001; Aschenbrenner et al. 2013). The addition of a dichloromethane solution containing the esterified cellulose into a large volume of ethanol facilitated the formation of micro and nanostructures with distinct shapes due to the supersaturation of the solution in the dichloromethane/ethanol mixture. The most fascinating observation is how manipulation of the addition rate of the cellulosic solution, the particle concentration, and the volume ratio of the dichloromethane to the antisolvent can be used to control the formation of nanospheres (Fig. 2a). For example, low volumes of ethanol to dichloromethane resulted in the formation of extended network structures (Fig. 2c). A minimum ratio of 10:1 ethanol/dichloromethane was needed to ensure the formation of spherical nanoparticles. In addition, it was determined that initial cellulosic concentrations of 1% w/v or lower, and addition rates slower than 20 mL/h were essential. Outside these parameters, the morphology of the particles was less uniform and a mixture containing structures that resemble cellulose

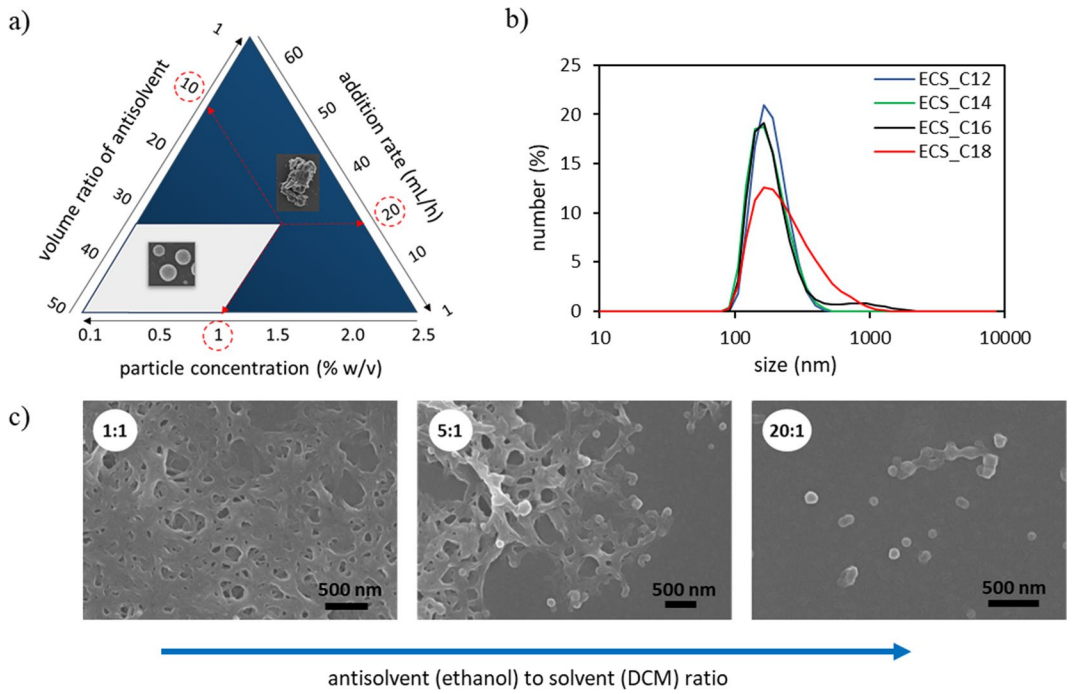

Fig. 2 (**a**) Optimization of parameters for the synthesis of ECS. (**b**) Determination of the particle size distribution of ECS using dynamic light scattering. (**c**) SEM images of the products formed from the nanoprecipitation of ECS_C18 using different antisolvent (ethanol) to solvent ratios (DCM)

nanocrystals and nanofibrils were formed (see SI, Sect. 2). In line with these results, previous studies have demonstrated that high antisolvent-to-solvent ratios and low initial solute concentrations enhance homogeneous nucleation during the formation of nanoparticles (Kakran et al. 2010; Thioune et al. 1997; Beck-Broichsitter et al. 2010; Aubry et al. 2009). These conditions reduce the interaction of seeding nuclei as they are more distant, thereby limiting aggregation and facilitating the growth of nanoparticles with controlled morphology.

The morphology of the nanospheres did not differ significantly upon esterification with acyl chlorides of different carbon chain lengths (See SI, Section 2c). The particle size distribution, as measured by dynamic light scattering, is uniform among the series of ECS with an average nanosphere diameter of around 160 nm (Fig. 2b). The broader size distribution of ECS_C18 observed under DLS is likely due to agglomeration of particles. This is corroborated by the SEM images (SI, Section 2c) which show that the ECS_C18 particles have similar aspect ratios and particle sizes compared to the other series of particles. It was observed that the nanospheres containing longer chains tend to aggregate to a greater extent. This behavior is likely due to the lower affinity of these particles with ethanol, which was used as the solvent for the imaging. Longer carbon chains can induce a higher degree of aggregation as has been seen in prior studies (Wen et al. 2017; Pang et al. 2018).

Surface characteristics of the esterified cellulose nanospheres

Previous studies have found that particle wettability can greatly affect particle-interface interactions as particles of different wettabilities display different affinities to the interface (Ballard et al. 2019). The addition of long carbon chains to the surface of our particles is likely to change their wettability; therefore, measurements of the static contact angle of water on substrates coated with ECS were taken to analyse the hydrophobicity of the nanospheres (Fig. 3a). The obtained contact angles were all greater than 90°, indicating a hydrophobic particle surface. In addition, ECS_C18 exhibited superhydrophobic behaviour, with the highest contact angle of 156° ± 4° (Parvate et al. 2020). It is well-established that the adsorption of hard particles to the interface of two immiscible liquids can reduce the interfacial area and energy of the system (Binks 1998). To understand the effect of hydrophobic cellulose nanospheres dispersed in a water-hexane mixture, the interfacial tension was measured (Fig. 3b). A reduction in interfacial tension was observed in the presence of the hydrophobic nanospheres, with an effect that was proportional to the length of the alkyl chain. For instance, the interfacial tension decreased from 45.8 mN/m in the control without particles (red dashed line) to 35.7 mN/m and 31.1 mN/m in the presence of cellulose laurate (shortest chain) and stearate (longest chain), respectively. This finding suggests that esterified cellulose containing longer alkyl chains decreases to a greater extent

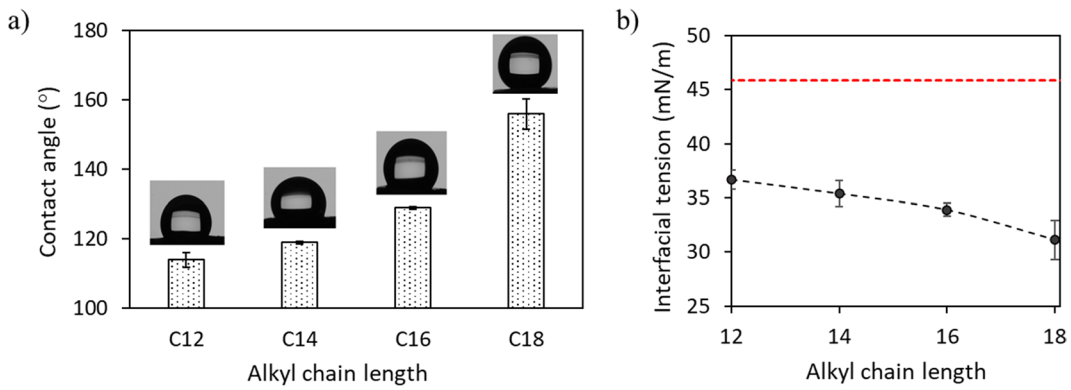

Fig. 3 (**a**) Static contact angle of water on substrates coated with ECS. (**b**) Interfacial tension of water/hexane in the presence of ECS_C12, ECS_C14, ECS_C16, and ECS_C18. The red dotted line represents the interfacial tension of water/hexane in the absence of any additives

the energy of the water-particle-hexane interface, which is one of the key factors that affect the adsorption and stability of particle-laden interfaces (Ballard et al. 2019).

Pickering emulsions stabilized with cellulose ester nanospheres

Having established that the cellulose ester nanospheres are able to adsorb to the hexane-water interface and reduce its interfacial energy, the formation of Pickering emulsions was investigated. Our nanospheres were compared for their ability to form 3:7 water-in-hexane emulsions by determining the EI%, which compares the emulsion height to the total system height (Willumsen and Karlson 1997). The concentration of particles is known to play an essential role in the stabilization of Pickering emulsions (de Carvalho-Guimarães et al. 2022; Juárez and Whitby 2012); therefore, emulsification was attempted with concentrations from 0.1% w/v to 2% w/v (Fig. 4a). The drop dilution test revealed that ECS_C12, ECS_C14, ECS_C16, and ECS_C18 promoted the formation of W/O Pickering emulsions, exhibiting miscibility in hexane (SI, Section 3a). This finding is in line with other studies in this area, indicating that hydrophobic particles exhibiting water contact angles higher than 90° tend to form W/O emulsions rather than O/W emulsions due to their higher oil-wettability (Choi et al. 2023). A comparison with hydrophilic cellulose spheres was carried out using the same conditions, which resulted in the formation of O/W emulsions, and the particles were not able to efficiently emulsify the system (SI, Section 3b). Although all four esterified nanospheres formed W/O Pickering emulsions, their EI% varies significantly. The

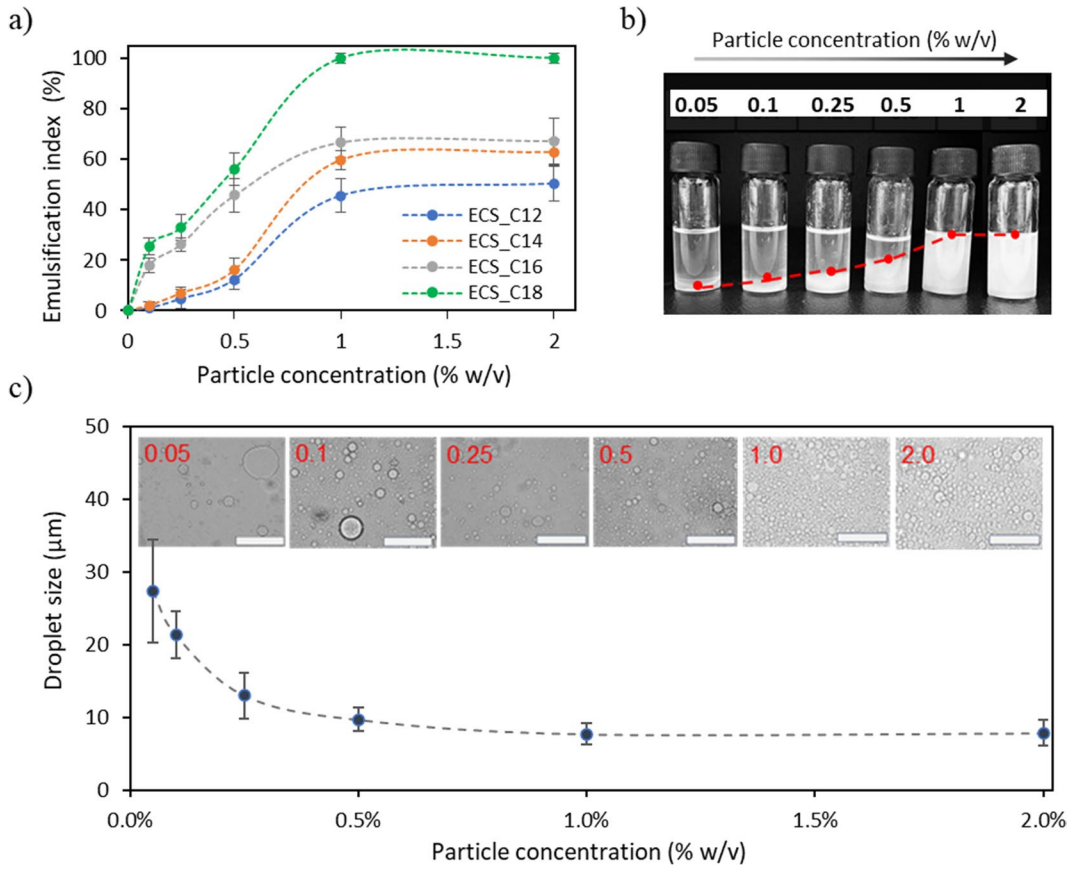

Fig. 4 EI% of water-in-hexane (3:7) emulsions stabilized with ECS at different particle concentrations. b) Image of the water-hexane mixtures with different concentrations of ECS_C18, taken 5 min after mixing. c) Average droplet size of the emulsions formed with ECS_C18. Bar size = 50 µm

emulsion stabilized with ECS_C12 showed the lowest EI% of 51% after reaching a plateau at a concentration of 1% w/v. On the other hand, the emulsions stabilized with ECS_C14 and ECS_C16 showed slightly improved EI% of 64% and 68%, respectively, which was constant after the addition of 1% w/v of nanoparticles. The change in the EI% of ECS_C14 began with an index similar to the emulsions stabilized with ECS_C12 at lower concentrations and increased in efficiency at higher concentrations to almost match the performance of ECS_C16. The nanospheres displaying the best emulsification performance were ECS_C18, as the EI% reaches 100% above a concentration of 1% w/v (Fig. 4b). A possible reason for the more efficient emulsification when longer chain lengths are used could be the presence of some aggregation of particles dispersed in the hexane, causing an increase in the viscosity of the oil, which would inhibit droplet sedimentation. The greater the mismatch between the chain length of the chains coating the cellulose particles and the hexane could enhance particle aggregation and hence the viscosity increase.

In addition, the EI% shows a rapid increase from a concentration of 0.1% w/v. Analysis of the droplet sizes in the Pickering emulsions formed using different concentrations of EC_C18 shows a correlation between the particle concentration and the average droplet size (Fig. 4c). At the lowest particle concentration of 0.05% w/v, droplet sizes with the largest average diameters of 27.3 ± 7 µm are formed, which decreases as the concentration is increased until reaching a plateau from a concentration of 1% w/v with an average droplet size of 7.7 ± 3 µm. Previous studies evaluating the particle concentration in Pickering emulsions have observed similar trends (Melle et al. 2005). Since the stability of this type of emulsion depends on effective coverage of the dispersed droplets by solid particles, higher particle concentrations allow an increase in the surface area, forming smaller droplets. However, once the minimum drop size is reached, excess particles can result in the formation of multilayer barriers or network structures (Sun et al. 2022). Our observations suggest that a particle concentration of at least 1% w/v is necessary to achieve complete water-hexane (3:7) emulsification with our ECS.

To provide further insight into the ability of the different ECS to stabilize water-in-hexane Pickering emulsions, optical micrographs of the emulsion were obtained using a particle concentration of 1% w/v (Fig. 5a). The emulsion formed with ECS_C12 (Fig. 5b) showed the smallest average droplet sizes of 3.9 ± 2.5 µm, with two main populations at 3.1 µm and 9.0 µm. The average droplet size increases to 4.2 ± 1.8 µm for the emulsion stabilized with ECS_C14, with a significant population at 5.9 µm (Fig. 5c). The emulsions formed with ECS_C16 exhibited a further increase in size to 5.4 ± 2.2 µm, with the size distribution showing two major peaks at 3.5 µm and 6.0 µm (Fig. 5d). The largest average droplet size of 7.6 ± 1.4 µm was observed for the emulsions stabilized with ECS_C18 (Fig. 5e), with an unimodal distribution evident from both the micrograph and the size distribution. Generally, smaller droplet sizes result in emulsions that are more stable against sedimentation (Frelichowska et al. 2010; Chen et al. 2018; Kim et al. 2016). We speculate that the droplet size distribution for this emulsion was initially bimodal for our less stable emulsions formed with ECS_C12 and ECS_C14, but the population of larger drops rapidly coalesced after the emulsions were formed. Therefore, the high concentration of smaller droplet sizes observed in the microscope images is likely due to the fact that the larger droplets have already coalesced to produce much larger drops of water outside the emulsion. This is evidenced by the grayish layer below the turbid emulsion layer for ECS_C12 (Fig. 5a). In contrast, the emulsion stabilized by ECS_C18 has a higher density of droplets, indicating that coalescence has not yet occurred.

To gain further insight into the limits of the water-in-hexane Pickering emulsions formed with our hydrophobic particles, the volumetric water/oil ratio was increased to 1:1 and 7:3. The emulsions formed with ECS_C18 (Fig. 6) show that a high emulsification index is still obtainable when mixing similar volumes of water and hexane, though this is reaching the limit of its emulsification ability as a small layer of hexane is observable at the top of the 1:1 emulsion. However, a system with a higher volume of water (7:3) is detrimental to the emulsification with ECS_C18 since two layers were formed. A drop dilution test and the microscopic analysis of this two-layer system indicate that the upper layer consists of a W/O emulsion while the bottom layer is an O/W emulsion. This observation suggests that the maximum volume of the dispersed phase (water)

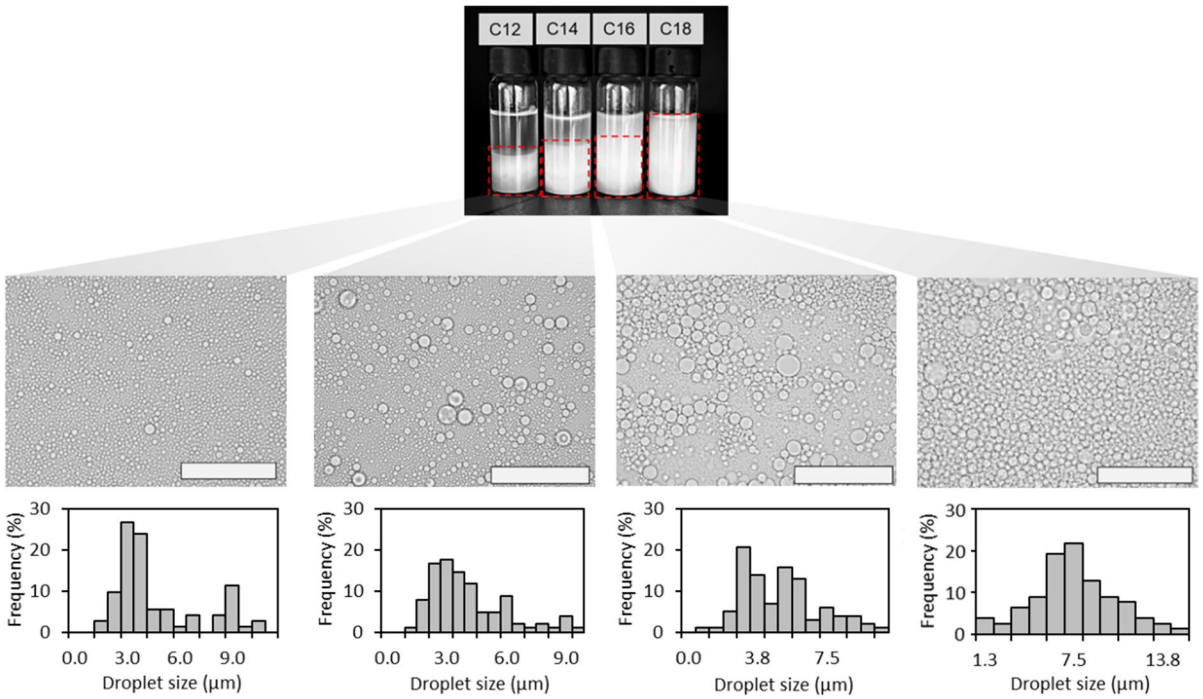

Fig. 5 Droplet size distribution and optical micrographs of the Pickering emulsions stabilized with (a) ECS_C12, (b) ECS_C14, ECS_C16, and d) ECS_C18. Bar size = 50 μm

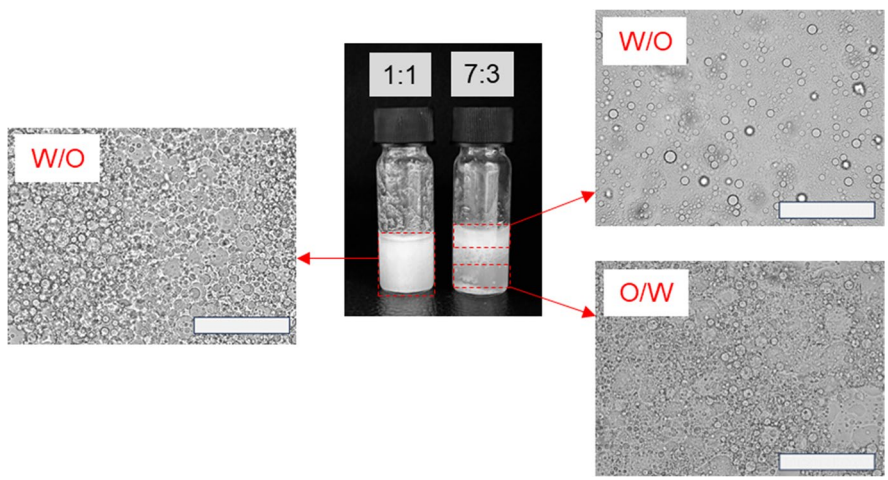

Fig. 6 Optical microscope images of the emulsions formed with ECS_C18 using water/hexane ratios of 1:1 and 3:7. Bar size = 50 μm

has been surpassed, resulting in catastrophic phase inversion due to the instability of the system (Binks and Lumsdon 2000). It is therefore likely that at this particle concentration, ECS_C18 can stabilize W/O systems of up to a volume ratio of 1:1 water in oil.

Comparison of emulsification action with a molecular surfactant

Having determined that the most effective W/O Pickering emulsifier was ECS_C18, its emulsification performance was compared to the molecular surfactant

Span® 60. This surfactant is a commonly used W/O emulsifier as it has a low HLB value of 4.7 due to its hydrophobic nature featuring an 18-carbon acyl chain attached to sorbitan. Emulsions were formed using ECS_C18 or Span® 60 with a concentration of 1% w/v, and changes in the EI% were monitored over 24 h (Fig. 7a). Under these conditions, Span® 60 was not able to form an emulsion with an EI of 100%, while this was possible with ECS_C18 (t = 0 h). Upon standing for 24 h, significant sedimentation was observed for the emulsion stabilized with Span® 60, and the EI% dropped from 79 to 18%. A lower degree of sedimentation was observed for the emulsion with ECS_C18, which dropped from 100 to 59% over 24 h. Upon closer inspection of the emulsion stabilized by ECS_C18 (t = 24 h), a gray layer was observed at the bottom of the vial, indicating the release of water due to coalescence and partial phase separation. This issue could be improved by utilizing ECS_C18 at a concentration of 2% w/v, which was able to more efficiently emulsify the 3:7 water/hexane mixture and exhibited a similar degree of sedimentation after 24 h when compared to Span® 60.

Conclusions

Although recent research shows increasing advances in the study of Pickering emulsions, few examples exist for the use of bio-based particles in W/O systems due to the lack of naturally occurring hydrophobic particles. In this study, we have demonstrated the generation of highly hydrophobic nanospheres by the esterification of microcrystalline cellulose and its controlled nanoprecipitation in an antisolvent. Formation of nanospheres with low aspect ratios and narrow size distributions required low initial cellulose concentrations (< 1% w/v), high volumetric ratios of antisolvent to solvent (> 10:1), and slow addition rates (< 20 mL/h). The resulting lauroyl-, myristoyl-, palmitoyl- and stearoyl-modified nanospheres are capable of reducing the interfacial tension of hexane/water, with an effect that increases with the length of the carbon chain on the acyl modifier. The stearoyl-modified nanospheres were determined to be superhydrophobic (contact angle 156° ± 4°), and reduce the interfacial tension of hexane/water from 45.8 mN/m to 31.1 mN/m. The enhanced oil-wettability allowed these particles to act as a water-in-hexane Pickering emulsifier with stability over time that compared favorably with the molecular surfactant Span® 60. The present study demonstrates the potential of bio-derived particles to act as efficient W/O emulsifiers and aims to inspire their potential use in applications such as cosmetic preparations, agricultural formulations, and foam production.

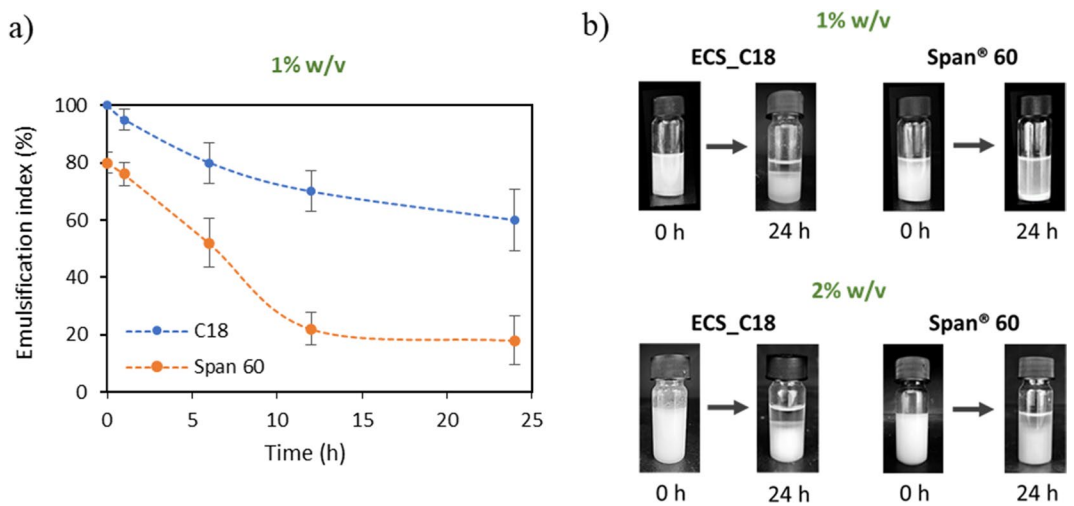

Fig. 7 (**a**) Time evolution of the EI% of water-in-hexane (3:7) emulsions stabilized with EC_C18 and Span® 60. (**b**) Images of the mixtures after 0 h and 24 h

Acknowledgements The authors thank Albina Avzalova for assistance with TGA measurements and Dr Yuan Tao for assistance with SEM imaging.

Author contributions BATA: Conceptualization, Investigation, Methodology, Writing – original draft. MMN: Investigation, Methodology. JVD: Investigation, Validation. OM: Investigation. CPW: Formal analysis, Writing – review & editing. JLYC: Methodology, Writing—review & editing, Supervision, Funding acquisition.

Funding Open Access funding enabled and organized by CAUL and its Member Institutions. This work was supported by funding from Callaghan Innovation as a National Science Challenge—Science for Technological Innovation Seed Project (AUTX1901), and as a National Science Challenge Impact Acceleration Project (SfTI-IAP02-AUT). Funding was received from the New Zealand Ministry of Business, Innovation & Employment's (MBIE) Endeavour Fund as a Smart Ideas project (AUTX2201). This project has also received support from the MacDiarmid Institute for Advanced Materials and Nanotechnology.

Callaghan Innovation, National Science Challenge, SfTI Seed Project, AUTX1901, New Zealand Ministry of Business, Innovation & Employment, Endeavour Fund, Smart Ideas, AUTX2201, Callaghan Innovation, National Science Challenge, Impact Acceleration Award, SfTI-IAP02-AUT.

Data availability The datasets generated or analyzed during this study are available from the corresponding author upon request.

Declarations

Ethical approval Not applicable.

Consent for publication All authors approved the final manuscript and submission.

Competing interests The authors declare no competing interests.

References

Anjali TG, Basavaraj MG (2018) Shape-anisotropic colloids at Interfaces. Langmuir 35(1):3–20. https://doi.org/10.1021/acs.langmuir.8b01139

Aschenbrenner E, Bley K, Koynov K, Makowski M, Kappl M, Landfester K, Weiss CK (2013) Using the polymeric ouzo effect for the Preparation of Polysaccharide-based nanoparticles. Langmuir 29(28):8845–8855. https://doi.org/10.1021/la4017867

Ashby NP, Binks BP (2000) Pickering emulsions stabilised by Laponite clay particles. Phys Chem Chem Phys 2(24):5640–5646. https://doi.org/10.1039/b007098j

Aubry J, Ganachaud F, Cohen Addad J-P, Cabane B (2009) Nanoprecipitation of Polymethylmethacrylate by Solvent Shifting:1. Boundaries Langmuir 25(4):1970–1979. https://doi.org/10.1021/la803000e

Aveyard R (2012) Can Janus particles give thermodynamically stable Pickering emulsions? Soft Matter 8(19). https://doi.org/10.1039/c2sm07230k

Ballard N, Law AD, Bon SAF (2019) Colloidal particles at fluid interfaces: behaviour of isolated particles. Soft Matter 15(6):1186–1199. https://doi.org/10.1039/c8sm02048e

Beck-Broichsitter M, Rytting E, Lebhardt T, Wang X, Kissel T (2010) Preparation of nanoparticles by solvent displacement for drug delivery: a shift in the ouzo region upon drug loading. Eur J Pharm Sci 41(2):244–253. https://doi.org/10.1016/j.ejps.2010.06.007

Binks BP (1998) Modern Aspects of Emulsion Science. https://doi.org/10.1039/9781847551474

Binks BP, Lumsdon SO (2000) Catastrophic Phase Inversion of Water-in-oil emulsions stabilized by hydrophobic silica. Langmuir 16(6):2539–2547. https://doi.org/10.1021/la991081j

Binks BP, Lumsdon SO (2001) Pickering emulsions stabilized by Monodisperse latex particles: effects of particle size. Langmuir 17(15):4540–4547. https://doi.org/10.1021/la0103822

Binks BP, Whitby CP (2004) Silica particle-stabilized emulsions of Silicone Oil and Water: aspects of Emulsification. Langmuir 20(4):1130–1137. https://doi.org/10.1021/la0303557

Chen Q-H, Zheng J, Xu Y-T, Yin S-W, Liu F, Tang C-H (2018) Surface modification improves fabrication of pickering high internal phase emulsions stabilized by cellulose nanocrystals. Food Hydrocoll 75:125–130. https://doi.org/10.1016/j.foodhyd.2017.09.005

Cherhal F, Cousin F, Capron I (2016) Structural description of the interface of Pickering emulsions stabilized by cellulose nanocrystals. Biomacromolecules 17(2):496–502. https://doi.org/10.1021/acs.biomac.5b01413

Choi J, Kim H, Lee H, Yi S, Hyun Lee J, Woong Kim J (2023) Hydrophobically modified silica nanolaces-armored water-in-oil pickering emulsions with enhanced interfacial attachment energy. J Colloid Interface Sci 641:376–385. https://doi.org/10.1016/j.jcis.2023.03.075

Costa C, Rosa P, Filipe A, Medronho B, Romano A, Liberman L, Talmon Y, Norgren M (2021) Cellulose-stabilized oil-in-water emulsions: structural features, microrheology,

and stability. Carbohydr Polym 252. https://doi.org/10.1016/j.carbpol.2020.117092
Daware SV, Basavaraj MG (2015) Emulsions stabilized by silica rods via arrested demixing. Langmuir 31(24):6649–6654. https://doi.org/10.1021/acs.langmuir.5b00775
de Carvalho-Guimarães FB, Correa KL, de Souza TP, Rodríguez Amado JR, Ribeiro-Costa RM, Silva-Júnior JOC (2022) A review of Pickering emulsions: perspectives and applications. Pharm 15(11). https://doi.org/10.3390/ph15111413
de Folter JWJ, Hutter EM, Castillo SIR, Klop KE, Philipse AP, Kegel WK (2013) Particle shape anisotropy in Pickering emulsions: Cubes and Peanuts. Langmuir 30(4):955–964. https://doi.org/10.1021/la402427q
Deng W, Li Y, Wu L, Chen S (2022) Pickering emulsions stabilized by polysaccharides particles and their applications: a review. Food Sci Technol 42. https://doi.org/10.1590/fst.24722
Dong H, Ding Q, Jiang Y, Li X, Han W (2021) Pickering emulsions stabilized by spherical cellulose nanocrystals. Carbohydr Polym 265. https://doi.org/10.1016/j.carbpol.2021.118101
Fan Z, Zhang L, Di W, Li K, Li G, Sun D (2021) Methyl-grafted silica nanoparticle stabilized water-in-oil Pickering emulsions with low-temperature stability. J Colloid Interface Sci 588:501–509. https://doi.org/10.1016/j.jcis.2020.12.095
Frelichowska J, Bolzinger M-A, Chevalier Y (2010) Effects of solid particle content on properties of o/w Pickering emulsions. J Colloid Interface Sci 351(2):348–356. https://doi.org/10.1016/j.jcis.2010.08.019
Gonzalez Ortiz D, Pochat-Bohatier C, Cambedouzou J, Bechelany M, Miele P (2020) Current trends in Pickering emulsions: particle morphology and applications. Engineering 6(4):468–482. https://doi.org/10.1016/j.eng.2019.08.017
Guo J, Du W, Gao Y, Cao Y, Yin Y (2017) Cellulose nanocrystals as water-in-oil Pickering emulsifiers via intercalative modification. Colloids Surf a 529:634–642. https://doi.org/10.1016/j.colsurfa.2017.06.056
He Y, Wu F, Sun X, Li R, Guo Y, Li C, Zhang L, Xing F, Wang W, Gao J (2013) Factors that affect Pickering Emulsions stabilized by Graphene Oxide. ACS appl Mater Interfaces 5(11):4843–4855. https://doi.org/10.1021/am400582n
Heinze D, Mang T, Popescu C, Weichold O (2016) Effect of side chain length and degree of polymerization on the decomposition and crystallization behaviour of chlorinated poly(vinyl ester) oligomers. Thermochim Acta 637:143–153. https://doi.org/10.1016/j.tca.2016.05.015
Horn D, Rieger J (2001) Organic Nanoparticles in the Aqueous Phase—Theory, Experiment, and Use. Angew Chem Int Ed 40 (23). https://doi.org/10.1002/1521-3773(20011203)40:23<4330::Aid-anie4330>3.0.Co;2-w
Hornig S, Heinze T (2008) Efficient Approach To design stable water-dispersible nanoparticles of hydrophobic cellulose esters. Biomacromolecules 9(5):1487–1492. https://doi.org/10.1021/bm8000155
Huang F-Y (2012) Thermal properties and Thermal degradation of Cellulose Tri-stearate (CTs). Polym 4(2):1012–1024. https://doi.org/10.3390/polym4021012
Juárez JA, Whitby CP (2012) Oil-in-water Pickering emulsion destabilisation at low particle concentrations. J Colloid Interface Sci 368(1):319–325. https://doi.org/10.1016/j.jcis.2011.11.029
Kakran M, Sahoo NG, Li L, Judeh Z, Wang Y, Chong K, Loh L (2010) Fabrication of drug nanoparticles by evaporative precipitation of nanosuspension. Int J Pharm 383(1–2):285–292. https://doi.org/10.1016/j.ijpharm.2009.09.030
Kalashnikova I, Bizot H, Cathala B, Capron I (2011) New Pickering emulsions stabilized by bacterial cellulose nanocrystals. Langmuir 27(12):7471–7479. https://doi.org/10.1021/la200971f
Kalashnikova I, Bizot H, Bertoncini P, Cathala B, Capron I (2013) Cellulosic nanorods of various aspect ratios for oil in water Pickering emulsions. Soft Matter 9(3):952–959. https://doi.org/10.1039/c2sm26472b
Kibbelaar HVM, Dekker RI, Morcy A, Kegel WK, Velikov KP, Bonn D (2022) Ethyl cellulose nanoparticles as stabilizers for Pickering emulsions. Colloids Surf a 641. https://doi.org/10.1016/j.colsurfa.2022.128512
Kim I, Worthen AJ, Johnston KP, DiCarlo DA, Huh C (2016) Size-dependent properties of silica nanoparticles for Pickering stabilization of emulsions and foams. J Nanopart Res 18(4). https://doi.org/10.1007/s11051-016-3395-0
Levine S, Bowen BD, Partridge SJ (1989) Stabilization of emulsions by fine particles I partitioning of particles between continuous phase and oil/water interface. Colloids Surf 38(2):325–343. https://doi.org/10.1016/0166-6622(89)80271-9
Li Z, Wu H, Yang M, Xu D, Chen J, Feng H, Lu Y, Zhang L, Yu Y, Kang W (2018) Stability mechanism of O/W Pickering emulsions stabilized with regenerated cellulose. Carbohydr Polym 181:224–233. https://doi.org/10.1016/j.carbpol.2017.10.080
Lin Y, Skaff H, Emrick T, Dinsmore AD, Russell TP (2003) Nanoparticle Assembly and Transport at Liquid-Liquid interfaces. Science 299(5604):226–229. https://doi.org/10.1126/science.1078616
Liu B, Li T, Wang W, Sagis LMC, Yuan Q, Lei X, Cohen Stuart MA, Li D, Bao C, Bai J, Yu Z, Ren F, Li Y (2020) Corncob cellulose nanosphere as an eco-friendly detergent. Nat Sustain 3(6):448–458. https://doi.org/10.1038/s41893-020-0501-1
Maim CJ, Mench JW, Kendall DL, Hiatt GD (1951) Aliphatic acid esters of cellulose. Preparation by Acid-Chloride-Pyridine Procedure. Ind Eng Chem 43(3):684–688. https://doi.org/10.1021/ie50495a033
Melle S, Lask M, Fuller GG (2005) Pickering emulsions with Controllable Stability. Langmuir 21(6):2158–2162. https://doi.org/10.1021/la047691n
Meng W, Sun H, Mu T, Garcia-Vaquero M (2023) Chitosan-based Pickering emulsion: a comprehensive review on their stabilizers, bioavailability, applications and regulations. Carbohydr Polym 304. https://doi.org/10.1016/j.carbpol.2022.120491
Niu F, Han B, Fan J, Kou M, Zhang B, Feng Z-J, Pan W, Zhou W (2018) Characterization of structure and stability of emulsions stabilized with cellulose macro/nano particles. Carbohydr Polym 199:314–319. https://doi.org/10.1016/j.carbpol.2018.07.025

Nunes S, Ramacciotti F, Neves A, Angelin EM, Ramos AM, Roldão É, Wallaszkovits N, Armijo AA, Melo MJ (2020) A diagnostic tool for assessing the conservation condition of cellulose nitrate and acetate in heritage collections: quantifying the degree of substitution by infrared spectroscopy. Herit Sci 8(1). https://doi.org/10.1186/s40494-020-00373-4

Pang B, Liu H, Liu P, Peng X, Zhang K (2018) Water-in-oil Pickering emulsions stabilized by stearoylated microcrystalline cellulose. J Colloid Interface Sci 513:629–637. https://doi.org/10.1016/j.jcis.2017.11.079

Parvate S, Dixit P, Chattopadhyay S (2020) Superhydrophobic surfaces: insights from theory and experiment. J Phys Chem B 124(8):1323–1360. https://doi.org/10.1021/acs.jpcb.9b08567

Pickering SU (1907) CXCVI.—Emulsions. J Chem Soc Trans 91(0):2001–2021. https://doi.org/10.1039/ct9079102001

Rehman A, Liang Q, Karim A, Assadpour E, Jafari SM, Rasheed HA, Virk MS, Qayyum A, Rasul Suleria HA, Ren X (2024) Pickering high internal phase emulsions stabilized by biopolymeric particles: from production to high-performance applications. Food Hydrocolloids 150. https://doi.org/10.1016/j.foodhyd.2024.109751

Silva CEP, Tam KC, Bernardes JS, Loh W (2020) Double stabilization mechanism of O/W Pickering emulsions using cationic nanofibrillated cellulose. J Colloid Interface Sci 574:207–216. https://doi.org/10.1016/j.jcis.2020.04.001

Sun Z, Yan X, Xiao Y, Hu L, Eggersdorfer M, Chen D, Yang Z, Weitz DA (2022) Pickering emulsions stabilized by colloidal surfactants: role of solid particles. Particuology 64:153–163. https://doi.org/10.1016/j.partic.2021.06.004

Tan Y, Xu K, Liu C, Li Y, Lu C, Wang P (2012) Fabrication of starch-based nanospheres to stabilize pickering emulsion. Carbohydr Polym 88(4):1358–1363. https://doi.org/10.1016/j.carbpol.2012.02.018

Tang C, Chen Y, Luo J, Low MY, Shi Z, Tang J, Zhang Z, Peng B, Tam KC (2019) Pickering emulsions stabilized by hydrophobically modified nanocellulose containing various structural characteristics. Cellulose 26(13–14):7753–7767. https://doi.org/10.1007/s10570-019-02648-x

Thioune O, Fessi H, Devissaguet JP, Puisieux F (1997) Preparation of pseudolatex by nanoprecipitation: influence of the solvent nature on intrinsic viscosity and interaction constant. Int J Pharm 146(2):233–238. https://doi.org/10.1016/s0378-5173(96)04830-2

Wen X, Wang H, Wei Y, Wang X, Liu C (2017) Preparation and characterization of cellulose laurate ester by catalyzed transesterification. Carbohydr Polym 168:247–254. https://doi.org/10.1016/j.carbpol.2017.03.074

Willumsen PA, Karlson U (1997) Screening of bacteria, isolated from PAH-contaminated soils, for production of biosurfactants and bioemulsifiers. Biodegradation 7(5):415–423. https://doi.org/10.1007/bf00056425

Wu J, Ma GH (2016) Recent studies of Pickering emulsions: particles make the difference. Small 12(34):4633–4648. https://doi.org/10.1002/smll.201600877

Xie D, Jiang Y, Li K, Yang X, Zhang Y (2022) Pickering emulsions stabilized by Mesoporous nanoparticles with different morphologies in combination with DTAB. ACS Omega 7(33):29153–29160. https://doi.org/10.1021/acsomega.2c03215

Yang H, Zhang H, Peng J, Zhang Y, Du G, Fang Y (2017a) Smart magnetic ionic liquid-based Pickering emulsions stabilized by amphiphilic Fe 3 O 4 nanoparticles: highly efficient extraction systems for water purification. J Colloid Interface Sci 485:213–222. https://doi.org/10.1016/j.jcis.2016.09.023

Yang Y, Fang Z, Chen X, Zhang W, Xie Y, Chen Y, Liu Z, Yuan W (2017b) An overview of Pickering emulsions: solid-particle materials, classification, morphology, and applications. Front Pharmacol 8. https://doi.org/10.3389/fphar.2017.00287

Zhai K, Pei X, Wang C, Deng Y, Tan Y, Bai Y, Zhang B, Xu K, Wang P (2019) Water-in-oil Pickering emulsion polymerization of N-isopropyl acrylamide using starch-based nanoparticles as emulsifier. Int J Biol Macromol 131:1032–1037. https://doi.org/10.1016/j.ijbiomac.2019.03.107

Zhang T, Xu J, Chen J, Wang Z, Wang X, Zhong J (2021) Protein nanoparticles for Pickering emulsions: a comprehensive review on their shapes, preparation methods, and modification methods. Trends Food Sci Technol 113:26–41. https://doi.org/10.1016/j.tifs.2021.04.054

Zhang Y, Bao Y, Zhang W, Xiang R (2023) Factors that affect Pickering emulsions stabilized by mesoporous hollow silica microspheres. J Colloid Interface Sci 633:1012–1021. https://doi.org/10.1016/j.jcis.2022.12.009

Zhu F (2019) Starch based Pickering emulsions: fabrication, properties, and applications. Trends Food Sci Technol 85:129–137. https://doi.org/10.1016/j.tifs.2019.01.012